Chapter 4

G_E^n experiment E02-013

Experiment E02-013 was carried out at Jefferson Lab from February 28 to May 11, 2006 to measure the electric form factor of the neutron. In this chapter the experiment setup and instrumentation needed to measure the interaction $^3\overrightarrow{\mathrm{He}}(\vec{e}', n)$ are described. First the experimental overview and relevant coordinate systems will be presented. Then a short summary of the beam and accelerator will be presented in section 4.3. The target and method of polarization is described in setion 4.4. In section 4.5 the spectrometer used to detect the electron and measure it's momentum is portrayed. The neutron arm, used to detect the coincident hadron, is described in section 4.6. Finally, the data acquisition software used for decoding and initial physics analysis is presented in section 4.7.

4.1 Experimental Overview

During the running period of E02-013, four kinematic settings were taken in six intervals, not including the time spent on commissioning the apparatus. Three separate polarized ^{3}He target cells were used for the measured asymmetry. For calibration purposes, a foil target (containing six carbon foils and one BeO foils), a reference cell (providing an empty cell target, hydrogen target, nitrogen target), and a setting with no target cell were used.

Big Bite optics calibrations and beam spot check were acheived using the foil target. The nitrogen target is used to determine the contamination in scattering events from N_2 in the ^{3}He cells. The hydrogen target was used to calibrate the momentum and yields of the elastic events for Big Bite and Big Hand. Additionally, the nitrogen and hydrogen targets are used to determine the dilution of the neutral sample by protons empirically, which is an important correction for the physics asymmetry.

Data taking took place in this experiment for several different settings dependent on target, beam energy, neutron arm location, and electron scattering angle. These are described in Table 4.1. Kinematic 1 will not be presented in this thesis, and kinematic 2(a) used two different settings for the neutron arm threshold. This change in threshold creates a difference in the neutron and proton detection efficiencies which are a key component in the empirical measurement of the dilution of the neutral sample by protons. This difference in efficiencies is calculated using a Monte Carlo.

4.2 Principle and Experiment setup

This experiment that place in Hall A of Jefferson Laboratory in Newport News, Virginia, USA. Jefferson Laboratory is the home of CEBAF, a continuous electron accelerator that can provide beam energies of 0.6 - 6 GeV [40] []. The three experimental halls, A, B, and C, can all receive beam simultaneously. Each hall contains various standard equipment detector systems that facilitate the types of experiments

Figure 4.1: Image of Jefferson Laboratory. Shown is the accelerator and the mounds over the three experimental halls. The mound to the left is Hall A.

name	kin 1	kin 2 (a)	kin 3 (a)	kin 2 (b)	kin 3 (b)	kin
Target Cell	Barbara	Dolly	Edna	Edna	Edna	Edn
Beam Energy (MeV)	1519	2637	3291	2641	3290	207
Q^2 GeV^2	1.2	2.5	3.5	2.5	3.5	1.
BB Angle ($\circ$)	56.26	51.59	51.59	51.59	51.59	51.5
NA Distance (m)	8	10	10	10	10	
Time Frame	2/28-3/09	3/09-3/24	3/24-4/17	4/17-4/24	4/24-5/02	5/02-5/0

Table 4.1: A table showing the running conditions, time, accumulated charge, and kinematics of the different measurements referred to here and elsewhere as kinematics or for short kin. Kinematic one includes both the commissioning time and the first measurement. The measurement of $Q^2 = 1.3$ and 1.7 GeV^2 provide a comparison of the polarized ^{3}He technique with previous recoil polarization data while the other two measurements extend the measured range of Q^2.

the halls were designed to accomplish. While the beam was provided similarly to other experiments in Hall A, the equipment used to make this measurement was a custom installation that included a large momentum acceptance spectrometer, Big Bite, a high efficiency segmented neutron detector, Big Hand, and a polarized ^{3}He target, which serves as a source of highly polarized neutrons. A general layout of the apparatus is shown in Figure 4.2.

Using simulations, the requirements for Big Bite and Big Hand were developed. To match Big Hand to Big Bite, the required acceptance for elastics was simulated, and then expanded to insure the acceptance of all events with at least $p_{m,\perp} = 150$ MeV. Because at $Q^2 = 3.5$ GeV^2 the desired hadron momentum is 2.6 GeV, the thresholds, shielding, and depth of the neutron arm were developed to maximize

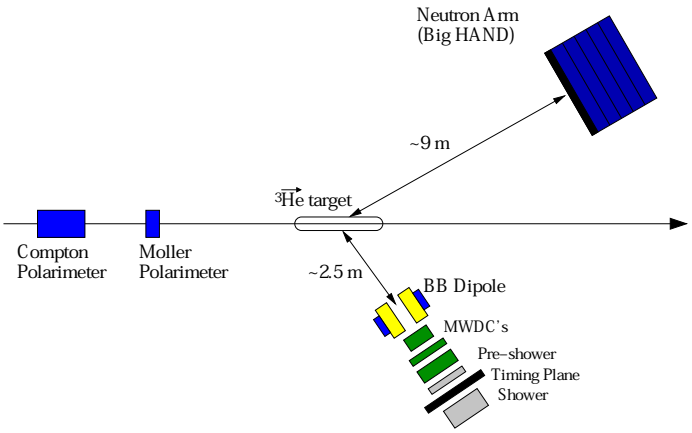

Figure 4.2: General layout, not to scale, of the experiment. Shown is the beamline, the target, the Big Bite detector stack, and the Neutron Arm detector. Also shown are the two polarimeters in the hall before the target, and the approximate distances to the detectors. The components of the Big Bite (BB) detector stack are also shown and consist of the Big Bite dipole magnet, multi-wire drift chambers (MWDCs), pre-shower, shower, and timing plane.

statistics. The desired Big Bite momentum resolution was 1-1.5% and the desired vertex resolution was 6 mm[16].

There were four major coordinate systems in this experiment: one for the lab, one for Big Bite, one for the target, and one for the Neutron Apparatus. In the hall system, the origin is at the center of the target, y is vertical with + as 'up', z is nominally along the direction of the beam, and x forms a right handed coordinate system. For the target coordinate system, the origin coincides with the hall origin, x is vertical with + as 'down', z is parallel to hall floor along the Big Bite central ray, and y completes the right-handed coordinate system. For the Big Bite detectors the origin is at the center of the first plane of the drift chambers. The $+z$ direction is defined in respect to the direction of particles perpendicular to the first drift chamber (and so is at a $\approx 10\circ$ angle with the $x-z$ plane in the lab frame),

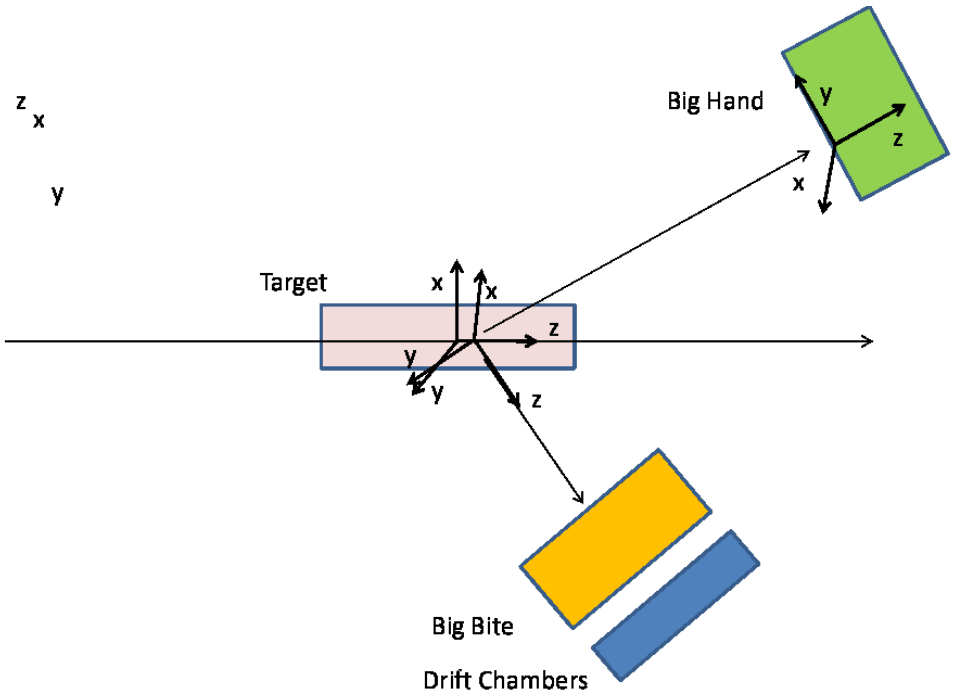

Figure 4.3: Coordinate systems for Big Hand, Target, and Lab. The lab z is along the beam line while the target z is toward Big Bite.

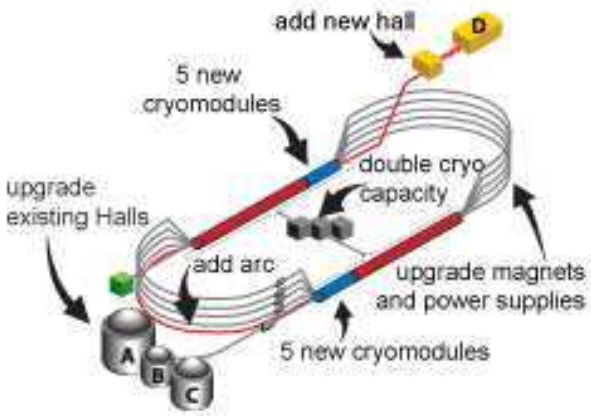

Figure 4.4: Schematic of the accelerator after the proposed 12 GeV upgrade. Shown are the three halls plus an additional proposed hall.

while $+x$ is in the magnetic dispersion direction, and y completes the right-handed coordinate system. In Big Hand, the depth is z, the height is x, and the horizontal position is y. In this coordinate system positive x is associated with 'down', positive z is associated with deeper into the Neutron Apparatus (NA), and positive y is away from the beam line. The origin was located in the center of the active area at the front of the shielding. Figure 4.3 shows the target, lab, and Neutron Arm coordinate systems and their relation to each other.

4.3 The Electron Beam

During 2006, the accelerator was capable of delivering beams with energy up to 5.7 GeV at currents of up to 150 μA semi-simultaneously to all three halls. The two main parts of the accelerator are the injector and the two recirculated linear accelerators (LINACs). These delivered beams are not quite continuous, rather the

beam was pulsed at a high rate of 499 MHz. Inside the injector, the lasers for each hall are 120 degrees out of phase compared to each other. This allows for the energy and current to be determined for each hall semi-independently. After the initial acceleration, a prebuncher and chopper make sure that the three individual beams are separated in time and longitudinal spread. After traveling through 18 superconducting radio frequency (SRF) cavities, the electrons are injected into the main accelerator at 23-68 MeV. See Figure 4.4 for a schematic of the accelerator.

Polarized electrons are produced from a strained GaAs photo-cathode via the photo-electric effect. A maximum polarizations of approximately 85% can be achieved. A Mott polarimeter at the injector can be used to measure the polarization using the asymmetry in the elastic Mott scattering.

The polarization of the high energy beam as it enters Hall A can be measured by a Compton polarimeter. This is done by scattering electrons from polarized photons, and measuring the asymmetry in the cross section due to the beam helicity change. The scattering takes place when electron beam interacts with a photon beam in a Fabry-Perot cavity (which enhances the yields). This method of measurement was used at the same time as data collection during kinematics two and three. On four separate occasions the beam polarization was measured by a Møller polarimeter in Hall A. This was done using magnetized foils which provide a target of polarized atomic electrons. The cross section was measured for two different orientations of the foil, and beam polarization was calculated using this. At various times during the experiment either of these two methods, or using the Mott polarimeter, were used to measure the polarization. This allowed for a good understanding of systematic

error for the beam polarization. An abridged summary of the beam polarization measurements is presented in Table 4.2.

The sign of the electron's helicity was put into the CODA data stream with a copy sent to the E02-013 trigger supervisor. The algorithm responsible produces helicity states (that last for a duration of 33.3 ms) in sets of four ($+--+$ or $-++-$). A 105 kHz clock was used to reconstruct the helicity if there was a problem with a missing helicity. After every transition there is a short unknown time where the helicity is unknown (given by 0) in the data.

In the Hall A beamline before the target, a set of field coils are located to move the beam to create a uniform pattern across a section of the cell. This is done so that a small portion of the target is not overheated and the target cell is not compromised. The beam sweeps through its pattern at a rate of 17 to 24 kHz in a process known as rastering. The current used to do this is read into the data stream, which allows the beam position to be calculated for this process.

Beam position monitors are presented upstream of the target (at 7.52 m and 1.29 m). The average position of the BPM is recorded at a rate of 1 Hz in EPICS. Upstream of BPMs is a fast rastering system (23 m). These BPMs were connected to an ADC for readout, such data could then be converted to a position for the beam. Harp scans were carried out to provide absolute position information which could be used to calibrate the positions. The BPM and raster calibrations were carried out by Brandon Craver and discussed in greater detail in another thesis [55].

During each pass, the two LINACs each accelerate the beam by up to 600 MeV during each pass. The beam can be bent and returned in RF cavities for up to

five passes through the LINACs. The beam is accelerated in the east and west and bent 180 degrees in the arcs. See Figure 4.4 for details of the accelerator setup and beam cavities. Because different electron energies need to travel through different magnetic fields to have the proper bend angle, the beam is split in a spreader and then recombined after traveling through the arc. Each cavity is also at 499 MHz to keep the beam properly bunched. The beam can be sent into the switch yard after any pass, where it is sent to hall A, B, or C. Beam energies were determined using the Tiefenbach method and recorded in EPICs. This method is that the energy of the electron beam is calculated by measuring the bend of the electrons as they pass through a magnetic field of one of the RF cavities.

4.4 The Helium-3 Target

Polarized targets and polarized ^{3}He have been used in previous experiments, as described in section 3.3.3. To review and expand upon this description, polarized ^{3}He targets are one of the preferred methods of realizing a polarized neutron target. As described, nuclei targets are used rather than free neutrons as the latter only survives with a halflife of 885.7 ± 0.8 s [1]. For polarization experiments ^{3}He is ideal as the polarization in the helium-3 is almost entirely carried by the neutron[1]. Additionally, the relatively simple nature of the ^{3}He nucleus allows final state interactions to be understood. These are thought to be small at high momentum transfer (section 5.7.1). In polarized ^{3}He, the neutron carries $\approx 86\%$ of the spin of the nucleus (Figure 4.5)[1]. Most of the time, the spins of the protons are in oppo-

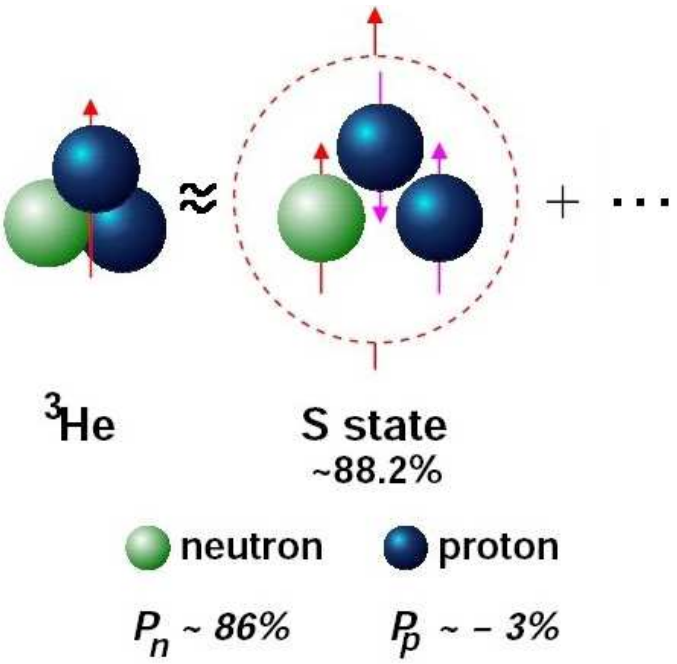

Figure 4.5: Diagram of the helium-3 nucleus. Shown is the most common state with the proton spins aligned anti-parallel. The neutron carries ≈ 86% of the polarization of the nucleus while the protons carry ≈ 3%.

site directions. About 3% of the time, the protons are polarized, and this proton asymmetry is corrected for when considering proton contamination of the neutral hadron candidates (see Section 5.5 and 5.6).

The process of spin-exchange optical pumping (SEOP) was used to polarize the ^{3}He nucleus. In this process alkali atoms are optically pumped and, through spin exchange, polarize the ^{3}He nucleus. An image of the target cell is provided in Figure 4.6. The process of SEOP will be described in section **??**.

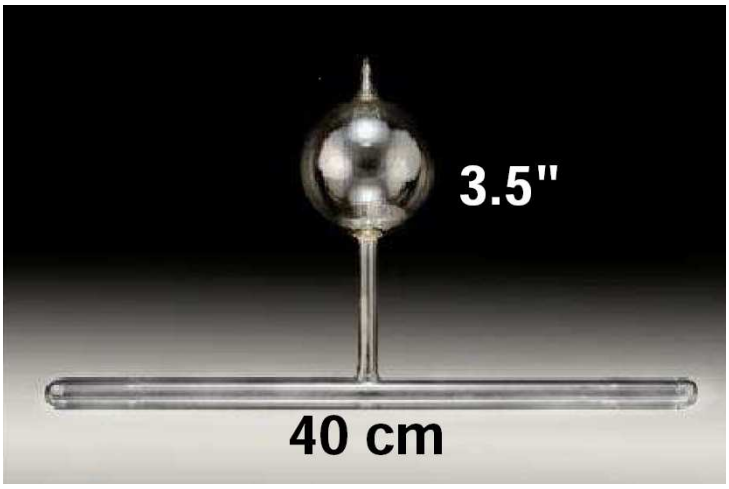

Figure 4.6: Picture of an empty ^{3}He cell. On top is the spherical pumping chamber, and below is the cylindrical target chamber. The beam passes through the the 40cm of target material[25].

4.4.1 Target System

The goal of the target system was to realize a polarized ^{3}He target. To have a polarized target, a magnetic field is required for the spin to be oriented with. To do this, the target system consists of a ladder holding the targets including a cell to hold the ^{3}He gas, a laser system to polarize the gase, and a system to create the uniform magnetic field.

The target system consisted of a ladder with four different targets and an iron box to provide a "constant" magnetic field in the target that is immune from interference due to the Big Bite dipole, and two polarimetry systems. The target cells were in a ladder system to change between $^3\overrightarrow{\text{He}}$, optics (carbon and beryllium oxide foils), reference cell (containing N_2 or H_2) targets. The reference cell was similar to the helium-3 cell and approximately 40 cm in length.

An oven was used to keep the pumping chamber at a constant temperature of 240◦ C. While 170◦ is all that is required to reach the desired density of Rubidium for spin exchange, 240◦ is required for the Potassium to be at sufficient density.

The target cell was made from hand-blown glass, with two chambers, a pumping chamber and a target chamber, and a transfer tube between the two. The polarized gas in the heated top chamber pumping would then diffuse into the bottom target chamber where the polarized ^{3}He served as the target. The cell was constructed of aluminesilicate glass and was filled with eight atm at room temperature of ^{3}He in addition to N_2 and sealed.

To optically pump the Rb, five 30 W lasers were used (totalling 150 W). In

order to decrease radiation damage and ease safety concerns, the lasers were not kept in the hall, rather they were kept in a shed with 75 m of optical fiber carrying the laser light to the target where it was combined in the pumping chamber.

All of the target system was held in an iron box, except the lasers. Around the target, there were coils to drive the RF field for the polarization measurements, and sets of pickup coils to measure the NMR signals, and a coil to provide the excitation for the EPR measurement (see Figure 4.10). The iron box and the holding field (25 G) it provided couldn't be too strong so as to not bend the beam away from the beam dump. The iron box provided shielding from Big Bite, with eight coils arranged to create a "uniform" field in the target region (Figure 4.8). The holding field wasn't completely uniform. Since the experiment is very sensitive to polarization direction this was measured using a specially built compass[39]. Figure 4.7 shows the relationship between position along the target and direction of the magnetic field.

4.4.2 Polarization

The ^{3}He target used in E02-013 was the first implementation of a hybrid target at Jefferson laboratory. The target's hybrid nature is due to containing two alkali metal vapor to reach a higher sustained polarization in less time than the previous mono-alkali targets. This target system was developed by Alan Gavalya and the polarized ^{3}He groups at the University of Virginia, the College of William and Mary, the University of Kentucky, and the Hall A staff. By using a Potassium

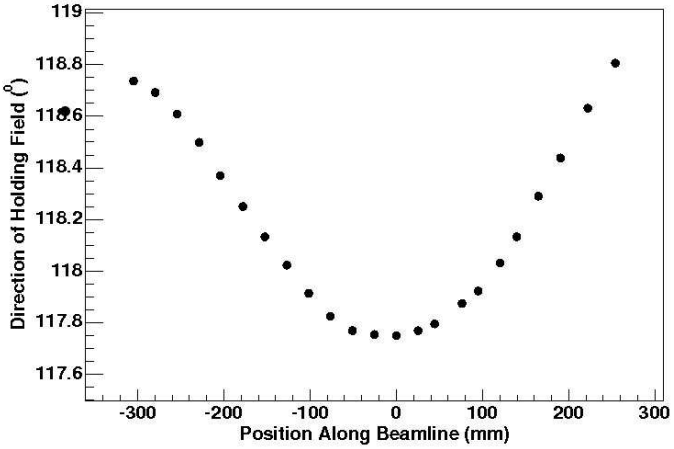

Figure 4.7: Measurement of the holding field as a function of position along the beamline in the target. The origin is the target center.

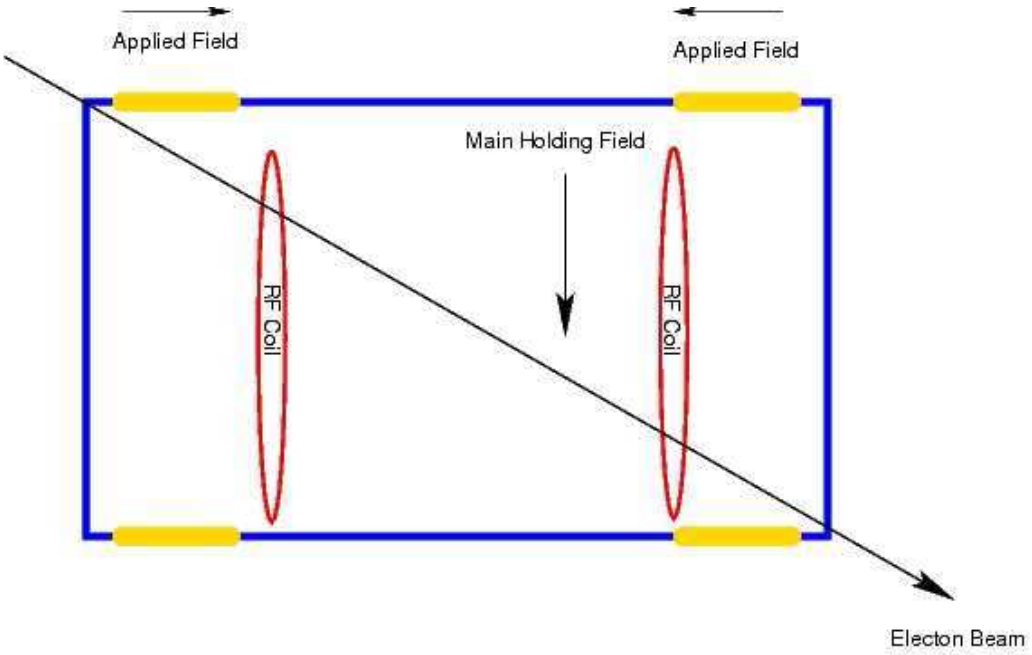

Figure 4.8: Magnet box for Target [36]. Shown is the coils that create the magnetic field.

and Rubidium mixture in the cells, a polarization higher than 50% was acheived (see Figure 4.11).

Rubidium is put in a magnetic field and exposed to the circularly polarized light, this pumps up the valence electron to a spin up sublevel in a P state. This excited state will either directly decay, or exchange spin through collision and then decay (see Figure 4.9). The photon released during decays can depolarize the nitrogen in the cells (roughly 2% of ^{3}He volume) serves to quench this, allowing the transition back to a bound state through kinetic collisions rather than radiation. After decay there is a 50% chance to end in a spin state. This spin state is not excited by light from the lasers and so becomes densely populated (see Figure **??**). Angular momentum can be transferred from the polarized alkali valence electron to ^{3}He via the hyperfine interaction. A description of these processes is presented in Figure 4.9.

The spin exchange efficiency for K-^{3}He interaction is 10 times more efficient than Rb-^{3}He. It is impossible to pump Potassium directly, as no commercial lasers of the proper wavelength exist. Potassium (K) and other alkali metals have a high spin exchange cross section with Rubidium and so the polarization of two such gases in a cell will be the same. This means that including the Potassium into the cell enhances the transfer of polarization into the helium-3, decreasing the time to polarize the cell by a factor of two and causing a corresponding increase in sustained polarization in beam.

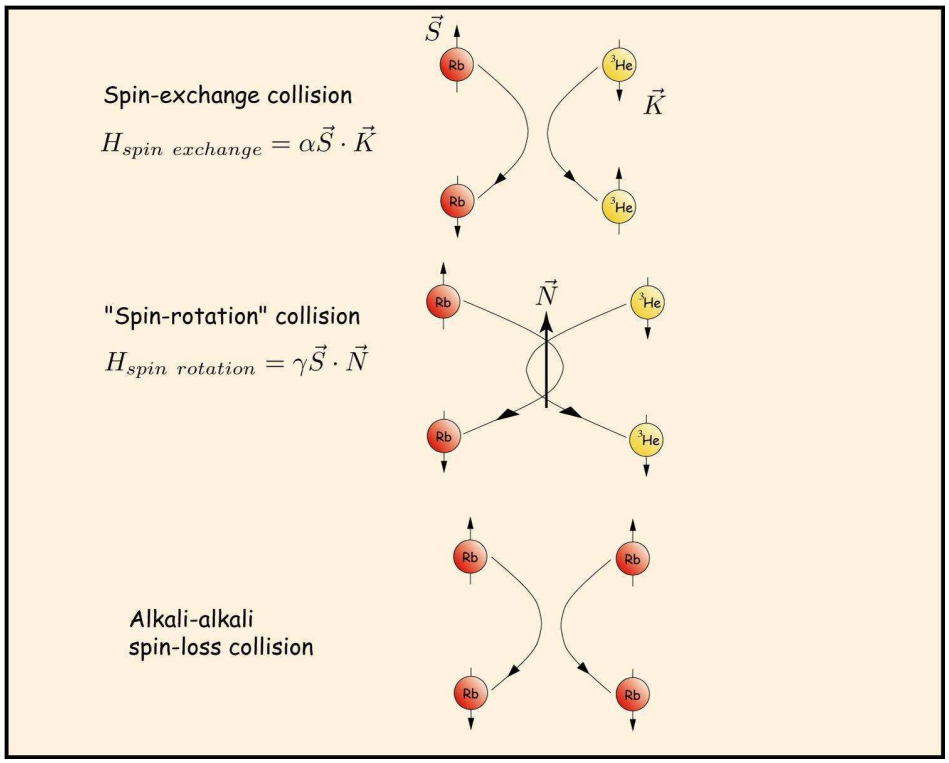

Figure 4.9: In a traditionally polarized Helium cell, one that contains only Rb and He, the Rb exchanges spin in one of three ways. Either by changing the spin of the He nucleus, or by just rotating the atoms it interacts with. This rotation is not useful for polarizing the He, so by adding K, which is liking to engage in 'spin rotation' with the Rb, but likely to engage in 'spin exchange' with He, the polarization efficiency of the cell is increased. Only the spin-exchange collision process causes polarization of the ^{3}He [64] [36].

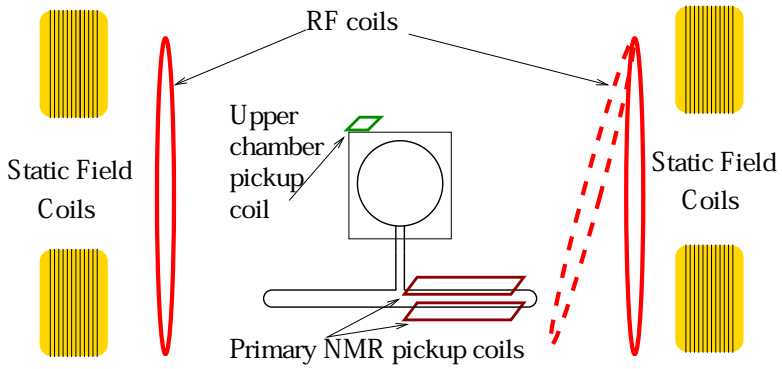

Figure 4.10: The coils used for the NMR measurement of target polarization. Shown is the holding field coils (iron box), the RF coils (which can be adjusted), and the pick up coils. Two sets of pick up coils are down at the target chamber, one more set is up above the pumping chamber. One of the RF coils could be adjusted, as could the pick up coils, to maintain the transverse relationships needed for an NMR measurement.

4.4.3 Polarization Measurement

The polarization of the target was measured by a combined use of EPR (electron paramagnetic resonance) and NMR (nuclear magnetic resonance) techniques. EPR provides an absolute measurement of ^{3}He polarization, while NMR provides a relative measurement. Both techniques cause depolarization of the target, but NMR disrupts the experiment less due to causing less depolarization. Because of this and that it was done in the target scattering chamber, NMR was done more frequently. These two techniques used two separate locations in the target cell. Due to using the alkali gases, EPR measured the polarization in the pumping chamber while NMR could be used to measure polarization in the target chamber. The diffusion of polarized gas in the cell was modeled to relate the two techniques and properly calibrate the NMR signal.

To do NMR, control of the magnetic field of the target is necessary. After an

application of a radio frequency (RF) field, when resonance conditions are met, a signal is measured that is proportional to the polarization of the target.

The resonance was found using adiabatic fast passage (AFP). In adiabatic fast passage the magnetic field is changed with a perpendicular radio frequency field (91 kHz) held constant to find the resonance. At resonance, ^{3}He undergoes spin reversal. This spin reversal produces an EMF signal that was detected in a separate set of coils known as pick up coils. See Figure 4.10 for a description of the coils involved in the NMR measurement.

This measurement technique switches the direction of the spins, so the magnetic holding field was swept back to give the original target polarization direction during each measurement. The depolarization caused by this process was found to be on the order of 1%. This measurement technique is relative due to the EMF signal depending on the magnetic flux through the coils, the amplification of the electronics, and the density of ^{3}He. The calibration of this measurement technique is presented in another thesis [35].

In an EPR measurement of the polarization of the ^{3}He, it is light from the polarization of the alkali metals in the cell that is measured. This is due to the alkali atoms being very sensitive magnetometers. This shift is due to the Zeeman effect. Obviously this means that there are two shifts in the Zeeman responses of the K and Rb, one due to spin exchange and another due to the magnetic field experienced by the metal including that of the polarized ^{3}He.

There are numerous magnetic fields which cause this shift, such as the holding field and interactions with the other atoms. However, these other shifts are not

dependent on the polarization of the target, and by flipping the polarization the effect due to the polarized ^{3}He on the magnetic field creating slight differences in the K energy levels can be determined. For a spherical sample, combining shifts due to collision and the classical magnetic field, the following relationship for the signal shift is obtained [32]

$$\Delta\nu_{EPR} = \frac{8\pi}{3}\frac{d\nu_{EPR}(F,M)}{dB}\kappa_0\mu_{He}P_{He} \ . \tag{4.1}$$

Here B is the magnet field, P_{He} is the polarization of the ^{3}He, and κ_0 is a parameter. To flip the target polarization, the holding field is kept constant and the applied RF field is swept (which is an resonance with the ^{3}He). The EPR resonance causes depolarization and florescence caused by that repolarization can be tracked as a function of RF frequency. This decay is caused by a shift in electron energy levels in the potassium atoms.

To understand the two measurement techniques relative to one another, NMR was done both before and after each EPR measurement. The EPR measurements had the disadvantage in causing significant target depolarization. This is because the EPR transition causes the ^{3}He spins to be anti-aligned with that of the spin state the alkali is being pumped into. To minimize the depolarization, this transition was done twice for every EPR polarization measurement. The EPR measurement depends on κ_0, which is different for every alkali and noble gas combination and has temperature dependence [59] [22].

The measurements required to relate the absolute EPR measurements and the relative NMR measurements and the model used to relate the polarization at the

different locations of the two measurements is presented in detail in another thesis [35]. The corrected polarization is shown in Figure 4.11. From equation 4.1 it is obvious that the target density neeeds to be known well. Resistive temperature devices (RTDs) were placed at eight locations on the cell to measure the temperature, the ideal gas law gave the density in the cell using this information. These RTDs did not measure the internal temperature, and so a series of NMR measurements were done under various conditions to determine the true internal temperature [35].

Many corrections are needed to provide the needed polarization and direction of polarization to properly determine the physical asymmetry. The material surrounding the helium-3 had to be understood to build a proper Monte Carlo, while the unpolarized nitrogen within the cell caused a dilution in the asymmetry. Details of these corrections are presented in section 5.5.2.

4.5 BigBite

4.5.1 The Big Bite Apparatus

Big Bite is the name of the electron spectrometer, and of the large 1.2 T dipole magnet that provides the magnetic field for the spectrometer. It consists of the large magnet, a plane of 13 scintillators, a calorimeter, and three multi-wire drift chambers (MWDC) containing a total of 15 wire planes. The calorimeter is split into a shower and preshower, and is constructed of 250 lead glass blocks. A schematic of the Big Bite detector is shown in Figure 4.12.

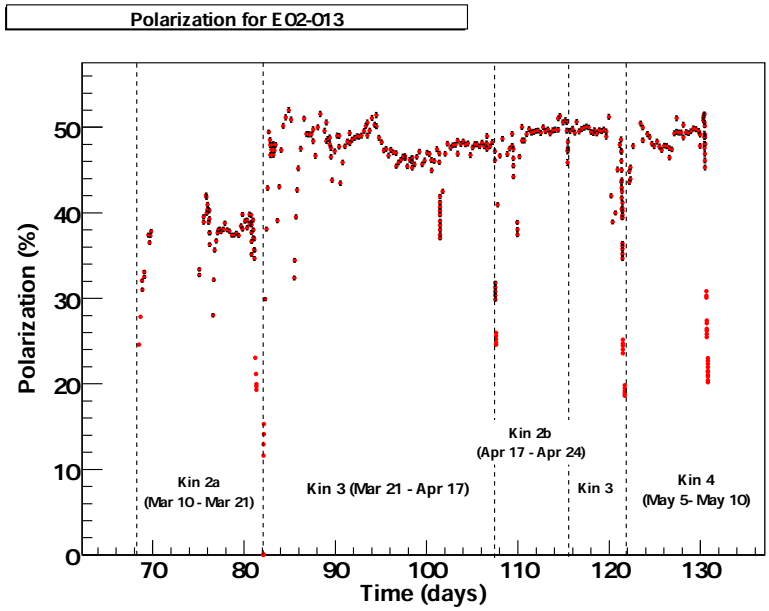

Figure 4.11: Measured polarization in the ^{3}He cells during the experiment [35]. Shown is all cells, including Dolly, Edna, and Barbara used during Kinematics 2, 3, and 4.

4.5.2 The Big Bite Scintillators and Shower

The Big Bite scintillators are located between the preshower and shower and provide the time of the event within Big Bite tracker. Each of the thirteen paddles has a photomultiplier tube on each end, with the signal split going to both a TDC via a discriminator and an ADC. The scintillators are used to calculate the time of the particle at the drift chambers, which are about one m away. The scintillator time, with resolution $\sigma = 300$ ps, is required for reconstructing the hadron time of flight due to its use in providing the reference time. These scintillators are 64 cm by 220 cm.

The front plane of the total shower, known as the pre-shower, which is one m behind the drift chambers is located behind the drift chambers. The preshower

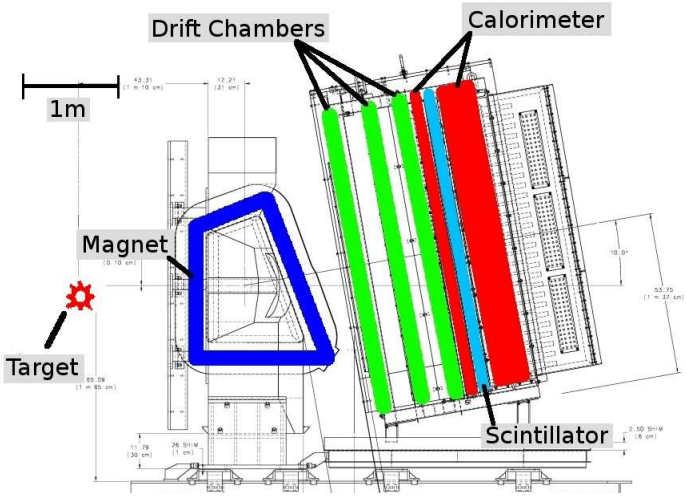

Figure 4.12: Schematic of the Big Bite detector. Shown is the large dipole which provides a magnetic field integral of 1.2 T·m, the 15 planes in three chambers that made up the wire chamber, and the lead glass shower and preshower with the layer of plastic scintillator between.

consists of 54 lead glass blocks in two columns of 27 rows. Behind the preshower, the shower consists of seven columns and 27 rows. The showers lead glass blocks are 8.5 cm by 8.5 cm, while the preshower has lead glass blocks that are 35 cm by 8.5 cm. The total height of the structure was 230 cm. Each block is connected to a single photomultiplier tube, which collects the Cerenkov light. The signal is then sent to both an ADC and summation module, with the summed signals going both to an ADC and a TDC. The sum of the shower and preshower gives a signal roughly proportional to the energy of the particle. The total shower provides the trigger for Big Bite. A final set of information provided by the total shower is the rough location of the particle. This aids track reconstruction in the multi-wire drift chambers and reduces the the search space by a factor of 10. The energy resolution provided by the total shower is approximately $\sigma_{\frac{dE}{E}} = 10\%$.

4.5.3 The Wire Chambers and Tracking

The drift chambers were constructed by the University of Virginia for this experiment in order to reconstruct the track that the electron travels through the detector. To do this, the planes which make up the drift chambers were constructed with three different orientations, known as U, X, and V. The chambers were roughly 35 cm apart. In the Big Bite detector coordinate system, the X plane has wires running parallel to the y axis, while the U and V wires are rotated by $\pm 30\circ$ in respect to that axis. The sense wires were one cm apart from each other within the plane. Cathode planes were placed three mm below above and below each wire

plane and field shaping wires were placed between each pair of sense wires to create a roughly symmetric potential around the sensing wires.

Charged particles which pass through the chamber release electrons by ionizing the gas within the chamber. This gas is a 50% argon and 50% ethane mixture that had been bubbled through ethyl and is kept slightly above atmospheric pressure. Since a voltage difference exists between the sense wires, the field shaping wires, and the cathode planes, the electrons are attracted to the detector wires and interact with them forming a signal which is then detected in a TDC (after amplification and discrimination). The time it takes to drift to the wire can be determined and used to calculate the distance between the wire and the particle track. Each plane was set at a different voltage to create the desired field surrounding the sensing wires.

The detector determines more than just the track that the particle traveled, it is also determines the particle momentum and from where along the target the particle originated. An effective bend plane model was used to determine this, where the interaction of the magnet is treated as occurring at the magnetic mid-plane. If we assume that there is only dispersion along Big Bite detector x, then the complete track between the target and the total shower can be reconstructed. By finding the point in the magnetic mid-plane that the observed track (back track) in the drift chambers points to, and assuming that dispersion happens only in the x (Big Bite) direction, the origin of the track along the beam (forward track) can be determined (V_0). All coordinates in this section are in the Big Bite detector coordinate system unless referred to as otherwise.

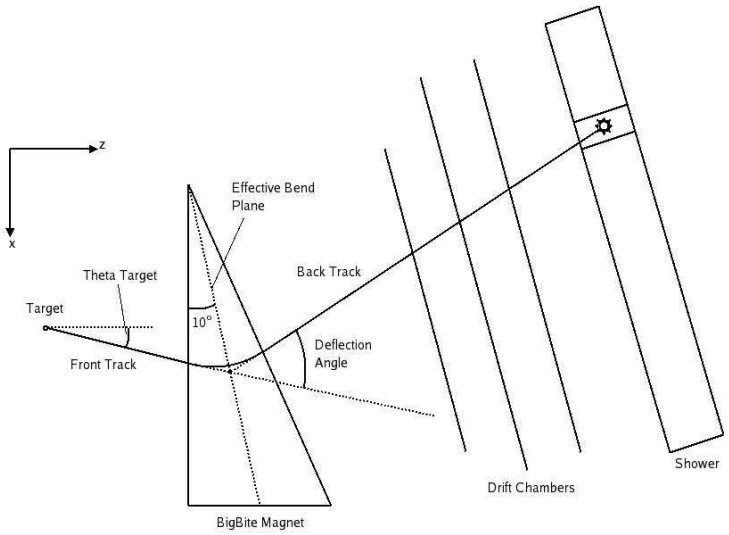

Figure 4.13: Not to scale diagram showing Big Bite, the location of the dipole, target, drift chambers, and shower, and the quantities known as the deflection angle (θ_{def}), θ_{tgt}, and the back and front tracks. Shown on the upper left is the coordinate system for the target coordinates. The shower is shown providing a fourth location for the particle, to anchor the track reconstruction. Big Bite detector coordinates have their origin at the center of the first plane. The z direction is perpendicular to the first chamber, and x is the magnetic dispersion direction.

In this model, the vertex is (after corrections $c_{x'}$, c_y, $c_{y'}$, and c_x)

$$V_{LAB} = c_0 V_0 + c_{x'} x' + c_{x_b} x_b + c_{y'} y' + c_{y_b} y_b + f(x_{bend}, y_{bend}) \tag{4.2}$$

Here the V is the z vertex location in the lab coordinate system, and $f(x_{bend}, y_{bend})$ is a parameter to determine deviations outside of this model. The x' and y' describe location of the intersection of the track with the plane $z = 0$ in the detector coordinate system. The variables $\Theta_{tgt} = x_b$ and $\Phi_{tgt} = y_b$ describe the track between the bend plane and the target and are found by $x_b = \frac{dx}{dz}$ and $y_b = \frac{dy}{dz}$ in the detector coordinate system. The bend coordinates (x_{bend}, y_{bend}) are the detector coordinates where the track intersects the bend plane. A diagram of the effective bend plane model is in Figure 4.13. A histogram showing the foil target vertex reconstruction is shown in Figure 4.15. This shows that the position along the target is reconstructed properly.

The momentum can also be determined, as

$$p_{BB} = \frac{c_0(x_{bend}, y_{bend}) + c_x x_{bend}}{\theta_{def}} + c_\theta \theta_{tgt} + c_y y + c_{y_b} y_b + f(x_{bend}, y_{bend}) \ . \tag{4.3}$$

This θ_{def} is the deflection angle, and defined using the vectors $\vec{x}_f$ and $\vec{x}_b$ which describe the tracks the particle takes between the target and the magnetic mid-plane and between the magnetic mid-plane and the wire chambers, and is defined to be

$$\theta_{def} = \cos^{-1}\left(\frac{\vec{x}_f \cdot \vec{x}_b}{|\vec{x}_f||\vec{x}_b|}\right) \tag{4.4}$$

The energy for the electron in elastic events can also be determined as

$$E_{elastic} = \frac{m_p E_e}{m_p + E_e\,(1 - \cos\theta_e)} \ , \tag{4.5}$$

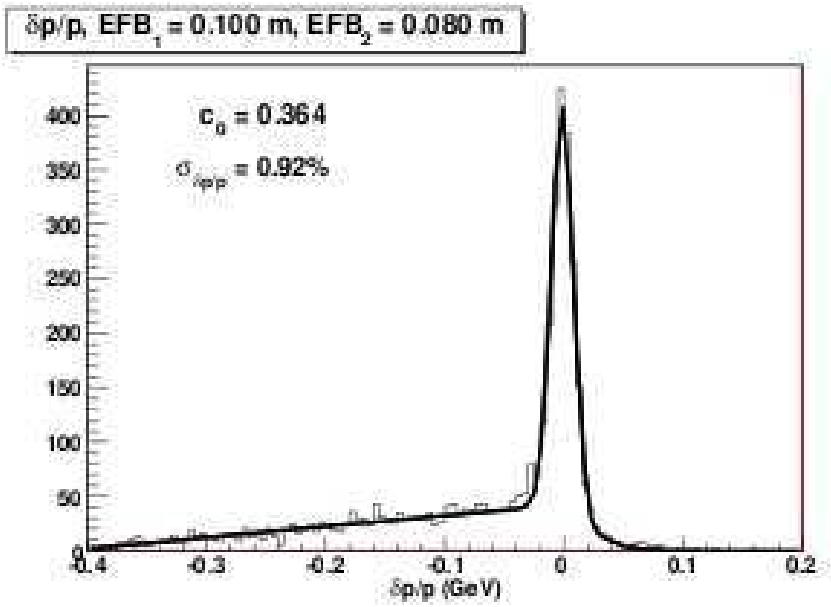

Figure 4.14: Momentum resolution achieved with the latest optics model.

where m_p is the mass of the proton and E_e is the energy of the electron, and θ_e is the electron scattering angle. These momentum calibration was done using hydrogen data. The momentum resolution is demonstrated in Figure 4.14.

4.5.4 Big Bite Electronics

Signals from each wire in the multi-wire drift chamber travel through an amplifier and discriminator before terminating at a LeCroy 1877 multi-hit TDC running in common-stop mode. Information is read out from these after each triggered. Different amplifier cards were used for each chamber. The scintillators have their signal split between a LeCroy 1881 ADC and a discriminator, with the discriminated signal terminating on a CAEN 775 TDC. The shower and preshower have all their

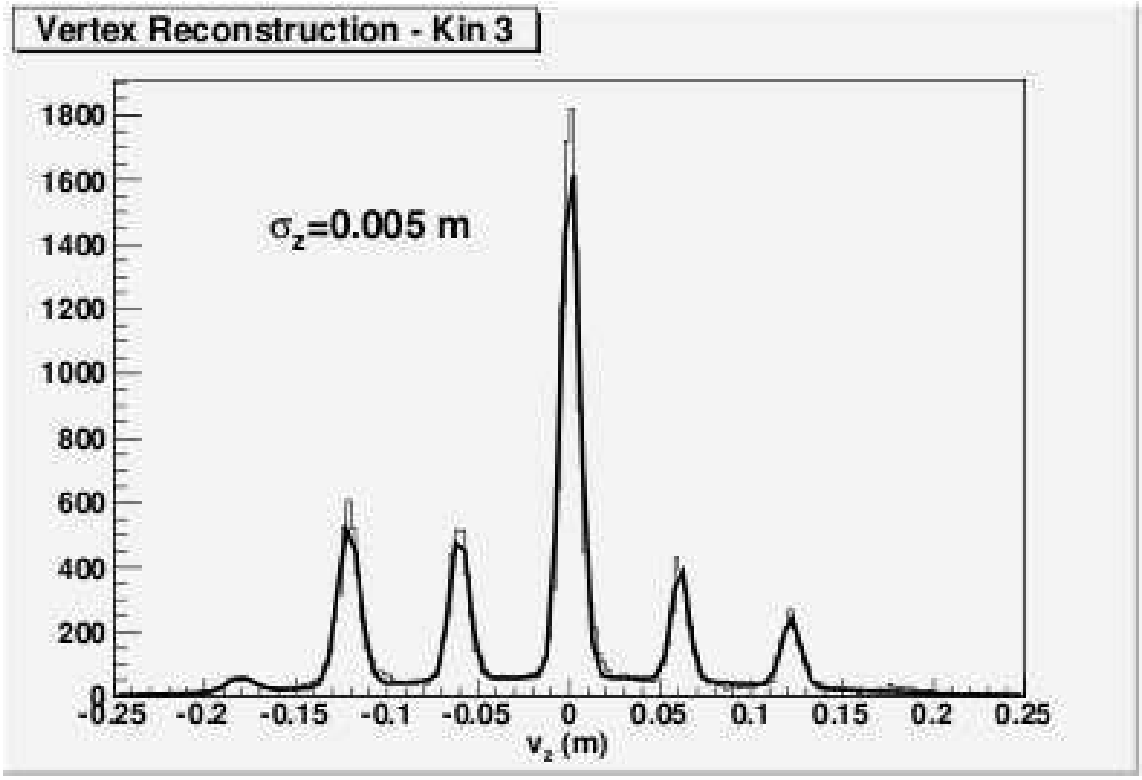

Figure 4.15: Resolution of the carbon foils after vertex corrections. Foils should be 6.7 cm apart with the BeO foil at zero cm. This is for a foil target run in kinematic 3.

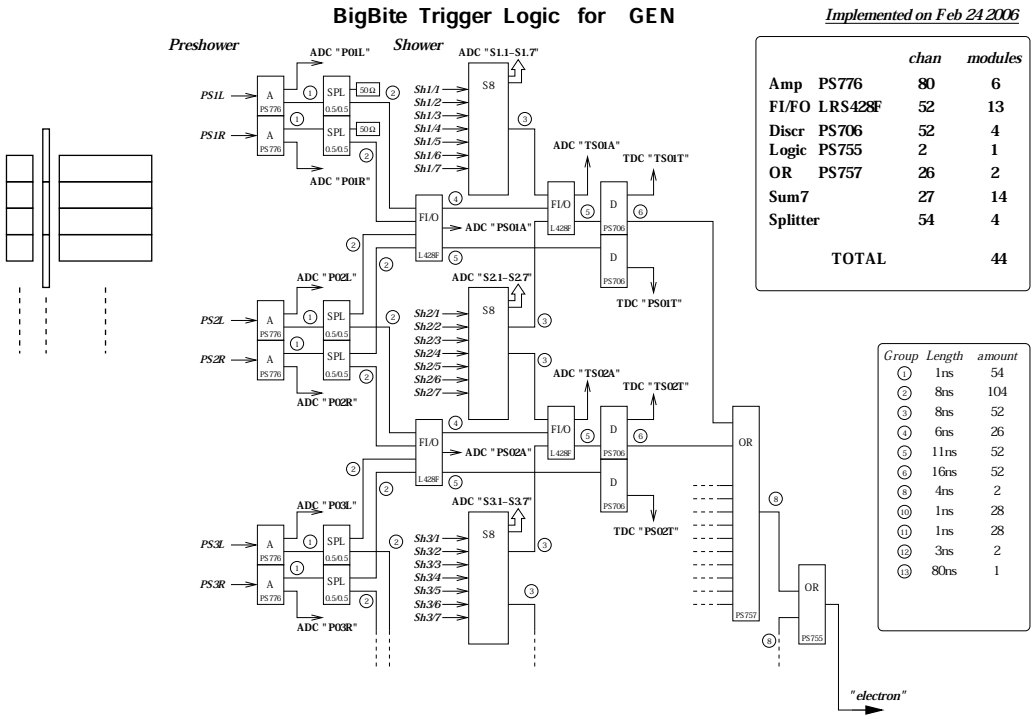

Figure 4.16: The electronics schematic for Big Bite. Shown are the modules and the wire lengths.

signals (individual and summed) put into a LeCroy 1881 ADC, with the sums also having the signal discriminated and put into a LeCroy 1877 TDC.

The sums of the preshower and shower that are over some predefined threshold provide the Big Bite trigger.

4.6 BigHand

While the subject of Big Hand is a major component of this thesis, the calibration and detailed analysis of the neutron arm's behavior is not needed directly for the analysis. As such, the geometry was described in detail in a document put together by Tim Ngo [47] and the software, detector description, analysis, and

calibration is presented in Appendix A.

4.6.1 Neutron Geometry

The neutron apparatus, sometimes referred to as Big Hand, is a large hadron detector, designed to match Big Bite's acceptance at the highest kinematic with $Q^2 = 3.5$ GeV^2. The dimensions of Big Hand are $4.2\times2.0\times6.2$m^3 and it has a 100 msr solid angle at a distance of eight meters. The neutron detector is made up of 244 neutron bars in seven planes and 192 segmented, single sided veto bars in two planes. These counters were provided by University of Virginia (UVA), University of Glasgow (GLA), and Carnegie Mellon University (CMU). In order to properly identify quasi-elastic events at the highest kinematic, a time resolution of 0.3 ns was desired which corresponds to neutron momentum resolution of 250 MeV/c at a hadron momentum of 2.58 GeV[16]. The scintillation material in the counters was the standard organic plastic scintillation material[]. To increase the detection efficiency of neutrons, a thin (one inch) layer of iron was placed in front of each counter to cause some portion of the incident neutrons to undergo hadronic interactions. A high degree of segmentation was important so that the vertical (X) position of the incident particle could be measured with the required resolution, this allows the selection of quasi-elastic events for which it is necessary to have a good measurement of momentum perpendicular to the virtual photon. Four 'marker' counters were included for calibration purposes.

4.6.2 Veto and Marker Bars

The veto counters were divided into two so that they would provide the needed time resolution without problems with attenuation. The two veto planes were offset from each other both horizontally and vertically, for complete coverage of the active area of the neutron bars. This, in addition to the height of veto bars (11 cm) compared to the neutron bars (15cm for CMU bars), meant that multiple veto bars could possibly fire to define the charge for an event within the neutron bars.

The marker counters were included late in the construction to calibrate the horizontal position reconstruction of the neutron detectors. These are long vertical scintillators placed before the first plane of the neutron detector, but after the shielding and veto detectors. They were placed within two constructed channels, with the same amount of space between the top marker bars and the bottom marker bars for each channel[46]. Even with two marker bars to cover the whole height of the neutron arm, most coincident hits between a marker bar and a neutron bar were only measured in a single PMT in the marker bar. Using these marker bars assisted in the time offset calibration of the neutron arm.

4.6.3 Neutron Arm Electronics

The initial discriminators, amplifiers, summing modules, were all placed in an electronics hut behind the neutron detector. The ADCs and TDCs were put behind shielding some 100 meters away, where the signals were discriminated again to provide a good signal. Signals from the detectors were combined into sums. This

was done to increase the neutron detection efficiency at $Q^2 = 2,5$ GeV^2. Figure 4.18 shows the neutron bars and veto bars, a sum is made up of the left or right PMTs for two neighboring color coded sections.

The ADCs used for the detectors within the neutron arm were all Lecroy 1881s, while the TDCs used for the veto detectors and sums were LeCroy 1877 TDCs. The F1 TDCs were specially developed electronics for Jefferson Lab and were used for the neutron counters. These TDCs were used in a common-stop mode and provided a resolution of 118 ps. The F1 TDC required that a reference signal be used, this was a delayed signal from the trigger and the F1 TDC signals could be reconstructed relative to it. Summing modules, amplifiers, fan in/out modules, discriminators, ADCs, TDCs are all presented in Figure 4.17 (and logic). This gives the NA side of the trigger as arising from any sum channel being past threshold on the left or right.

4.7 Data Acquisition

Six triggers were used in this experiment. These were neutron arm trigger (1) known as T1, the big bite trigger (2) known as T2, the coincidence trigger (3) known as T3, the 8.5 Hz pulser (7), the 105 kHz helicity synchronization signal (8), and the 30 Hz helicity quad duration signal (9).

The T3 trigger was formed by coincidence between the neutron arm and Big Bite. This coincidence was formed between any single sum channel on the neutron arm (left or right) and detection beyond a certain threshold in the preshower and

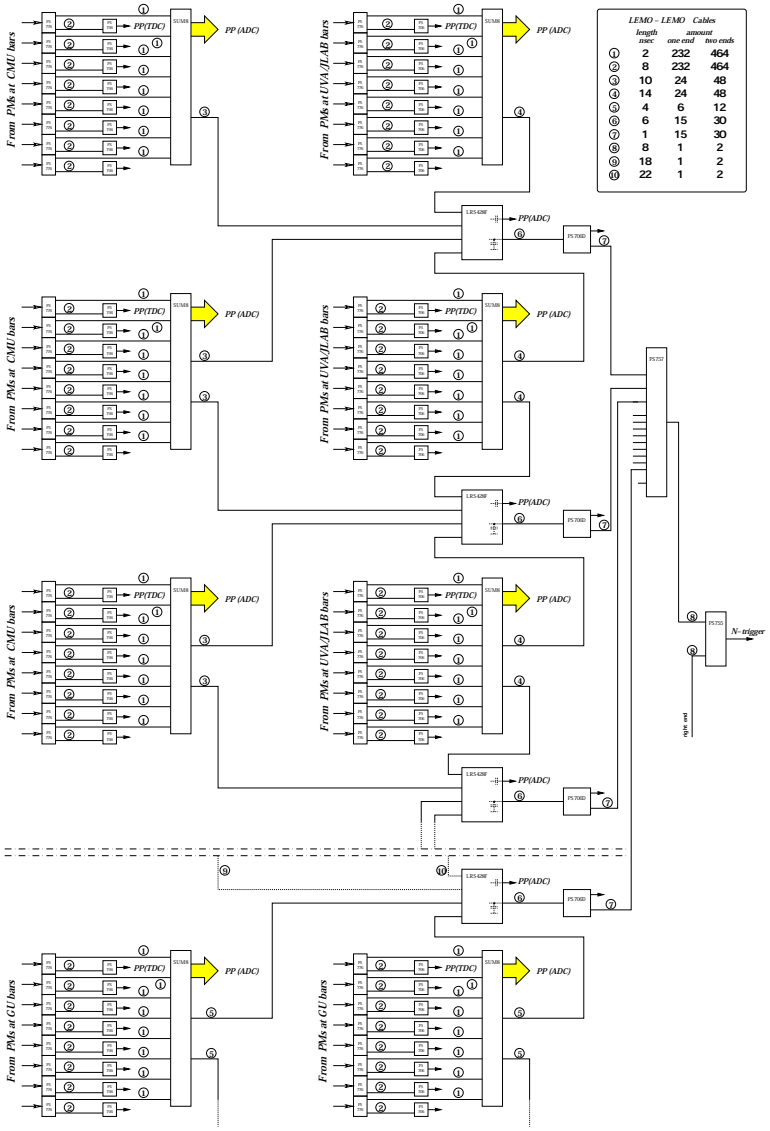

Figure 4.17: Neutron Arm electronics schematics. Included in the schematic is the length of the cables. From the PMTs of the various tubes, the signal goes into both a TDC and a sum module with the non-summed output going to an ADC. The different summed signals are added together and sent to both an ADC and TDC, with an OR of the TDCs forming the trigger.

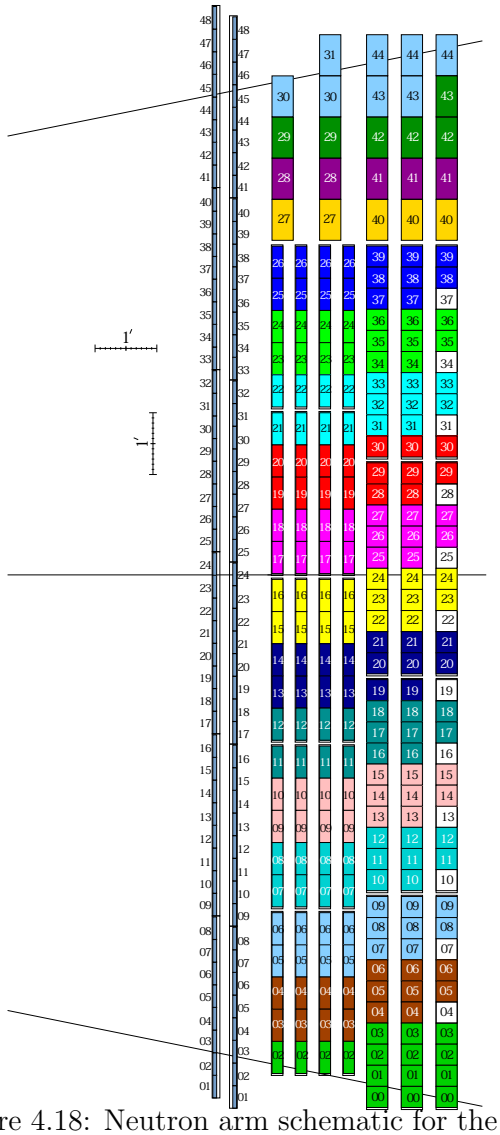

Figure 4.18: Neutron arm schematic for the sums. In front are the two veto planes. Shown is the relative offset. Additionally, color coded, the sums are shown. Each sum was made up of two neighboring color bands. Shown on top the bars from Glasgow (GLA), in the front are four planes of bars from Carnegie Mellon university (CMU), and in the back are three planes of bars from university of Virginia (UVA). The colorless bars in the final plane are bars that were not connected to the electronics. The first two thin planes are the veto planes, the figure shows the vertical shift between the two planes.

shower. In Figure 4.2 the grouping of neutron bars is presented. Two neighboring colors would be linked together to form one sum, with the left and right PMTs being considered separately. This was done to increase neutron detection efficiency at a higher threshold[53].

The time of the BigBite Shower was used for the time of the T2 trigger. The Big Bite scintillator time associated with this was then sent to the neutron arm to provide both the coincidence for the trigger and the reference time of the neutron arm events.

The neutron detector real time was recorded relative to a read out time or reference time. Thus the neutron arm recorded time was given as $t_{recorded} = t_{real} - t_{readout}$. The Big Bite trigger time relative to this same read out time was also recorded as $t_{L1A} = t_{readout} - t_{trig}$. The neutron arm time relative to the Big Bite trigger time is then $t_{real} = t_{recorded} + t_{L1A}$.

A trigger from both detectors, Big Hand and Big Bite, created a T3, the coincidence trigger. The $t_{readout}$ time was based on this T3 time. The T1 came 35 ns later than the T2 trigger due to delays added in. If the T1 came too early, $t_{readout}$ and T3 were based on on the T2 trigger. If the T2 trigger came very early, then the Big Bite readout was determined by $t_{readout}$ and not the T2 trigger. This is known as forced retiming. A plot showing the data with the different types of events is shown in Figure 4.19.

Both detectors provided information at each coincidence event. Single trigger events, were also taken but prescaled to provide a minimum number of events in the experiment. All three multi-wire drift chambers provide TDC information, the

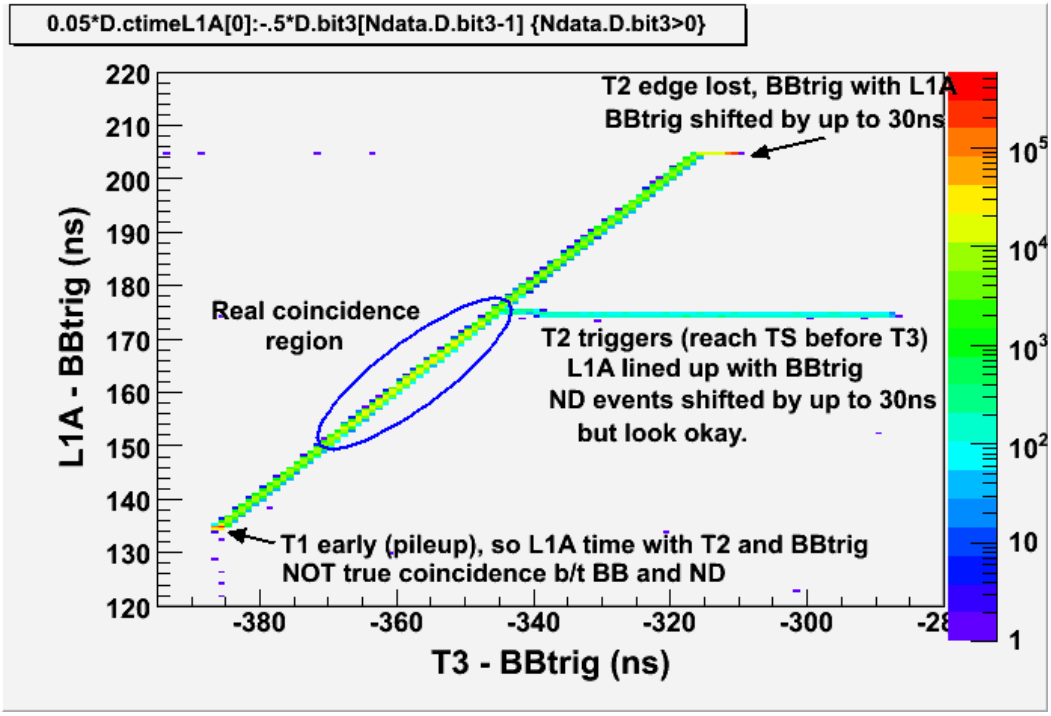

Figure 4.19: Plot showing the reference time and coincidence counts in relation to the Big Bite trigger time. Best coincident events are in the circled region.

scintillators provide both ADC and TDC, and the preshower and shower provided ADC information (with the preshower and shower sums providing TDC in addition to ADC information). All the neutron arm detectors provided both TDC and ADC information, with the neutron detectors also grouped into sums which provided ADC and TDC information as well. The neutron arm reference time was recorded in both the Neutron Arm TDCs and the Big Bite TDCs.

4.7.1 Encoding and Decoding

There are two main data acquisition systems. One is EPICS, which provides updates occasionally (no more often then every few ms) and provides information

about the target, accelerator, electronics, and scalars. This is included in the data stream with the events from the detectors. The events from the detectors is acquired using CODA, which can monitor, acquire, record, and decode data taken during experiments[31]. There was some target information which was stored separately.

To do the analysis and turn the raw data into usable information, a modification of the ROOT software package called the Hall A Analyzer was used[2]. This package has features which make it easier to deal with large amounts of data and to make histograms and graphs. Special classes for the analysis of the different detectors have been developed for the analysis of the neutron arm data and for tracking and momentum reconstruction in Big Bite and is discussed in other sections. The library which contains these classes is the AGen library[**?**]. The E02-013 experiment used a modification of this Hall A Analyzer. This was done so that in the decoding and initial calculation of physics quantities steps, the Big Bite tracking code could take advantage of other detectors. The scalar data were put in separate trees in this initial decoding and analysis of the data. During the initial decoding and analysis steps, the first 1000 events of a run were discarded (due to being helicity diagnostic events) as were non-coincidence events. During the decoding and even processing, the data is put into trees, which is a specific data format common for ROOT and are referred to as root files[60].

Date	Method	Polarization	Statistical	Systematic
March 30, 2006	Mott	83.32 %	1.45	1.00
March 30, 2006	Mott	81.62 %	1.45	0.98
April 13, 2006	Mott	84.12 %	1.11	1.01
April 13, 2006	Mott	83.25 %	1.11	1.00
Average	Mott	83.08 %	0.65	1.00
February 28, 2006	Møller	88.8 %	0.2	3.0
February 28, 2006	Møller	86.8 %	0.2	3.0
March 4, 2006	Møller	88.2 %	0.14	3.0
March 9, 2006	Møller	86.5 %	0.15	3.0
March 25, 2006	Møller	82.2 %	0.3	3.0
Average	Møller	86.5 %	0.09	3.0
April 18, 2006	Compton	82.92 %	2.31	2.40
April 20, 2006	Compton	85.63 %	3.87	1.55
April 22, 2006	Compton	86.47 %	1.63	3.55
April 24, 2006	Compton	82.65 %	1.64	3.20
Average	Compton	83.5 %	0	1.1 %

Table 4.2: A table of the beam polarization as measured by different means at different times. The Møller measurements were done in the Hall A Møller. The Mott measurements were done using the injector Mott measurement. Only selected Compton data is presented, the average is the averaged of all data for Compton.